AD-A051 497 NEW YORK UNIV N Y DEPT OF APPLIED SCIENCE F/G 20/4
THE EFFECTS OF ACOUSTICAL DISTURBANCES ON BOUNDARY LAYER TRANSI--ETC(U)
JAN 78 G MILLER, A CALLEGARI N00014-76-C-0183
UNCLASSIFIED NYU/DAS-78/01 NL

1 OF 1
ADA
051497

END
DATE
FILMED
4-78
DDC

NEW YORK UNIVERSITY

FACULTY OF ARTS AND SCIENCE

DEPARTMENT OF APPLIED SCIENCE

THE EFFECTS OF ACOUSTICAL DISTURBANCES ON BOUNDARY LAYER TRANSITION

G. Miller and A. Callegari

NYU/DAS #78/01

JANUARY 1978

ANNUAL REPORT

DEPARTMENT OF THE NAVY
OFFICE OF NAVAL RESEARCH

CONTRACT NO. N00014-76-C-0183

NEW YORK UNIVERSITY
FACULTY OF ARTS AND SCIENCE
DEPARTMENT OF APPLIED SCIENCE

Unclassified

SECURITY CLASSIFICATION OF THIS PAGE (When Data Entered)

REPORT DOCUMENTATION PAGE		READ INSTRUCTIONS BEFORE COMPLETING FORM
1. REPORT NUMBER	2. GOVT ACCESSION NO.	3. RECIPIENT'S CATALOG NUMBER
4. TITLE (and Subtitle) (6) THE EFFECTS OF ACOUSTICAL DISTURBANCES ON BOUNDARY LAYER TRANSITION.		5. TYPE OF REPORT & PERIOD COVERED (9) Annual ~~Technical~~ Rep[redacted]t. 9/15/75 to 12/15/77 15 Sep 75-15 Dec 77
		6. PERFORMING ORG. REPORT NUMBER (14) NYU/DAS-#78/01
7. AUTHOR(s) (10) Gabriel/Miller [redacted] Andrew/Callegari		8. CONTRACT OR GRANT NUMBER(s) (15) N00014-76-C-0183 new
9. PERFORMING ORGANIZATION NAME AND ADDRESS New York University/Department of Applied Science 26-36 Stuyvesant Street (Barney Bldg) New York, New York 10003		10. PROGRAM ELEMENT, PROJECT, TASK AREA & WORK UNIT NUMBERS NR 061-232
11. CONTROLLING OFFICE NAME AND ADDRESS OFFICE OF NAVAL RESEARCH/DEPARTMENT OF THE NAVY (CODE 430B)- 800 N. QUINCY STREET, ARLINGTON,VA. 22217		(11) 12. REPORT DATE 25 Jan[redacted]78
		13. NUMBER OF PAGES 30 (12) 36p.
14. MONITORING AGENCY NAME & ADDRESS(if different from Controlling Office)		15. SECURITY CLASS. (of this report) Unclassified
		15a. DECLASSIFICATION/DOWNGRADING SCHEDULE N/A
16. DISTRIBUTION STATEMENT (of this Report) Approved for public release; distribution unlimited		
17. DISTRIBUTION STATEMENT (of the abstract entered in Block 20, if different from Report) N/A		
18. SUPPLEMENTARY NOTES		
19. KEY WORDS (Continue on reverse side if necessary and identify by block number) Acoustical disturbances Boundary layer Transition Stability		

20. ABSTRACT (Continue on reverse side if necessary and identify by block number)

The analysis of transition from laminar to turbulent flow on a flat plate has been the subject of numerous investigations. In the present work, emphasis has been placed on establishing a computational technique which can be utilized to develop a basic understanding of the effects of the propagation of acoustic waves into a boundary layer, and the ultimate effect of such disturbances on transition. The nonlinear system of unsteady compressible partial differential equations have been solved by a MacCormack predictor-corrector scheme which allows the effects of imposed disturbances to be tracked in time. The question over

DD FORM 1 JAN 73 1473 EDITION OF 1 NOV 65 IS OBSOLETE

Unclassified

SECURITY CLASSIFICATION OF THIS PAGE (When Data Entered)

409 964

of the mismatch in propagation velocity between Tollmein Schlichting and acoustic waves has been studied. The program indicates that while disturbances are propagating with the speed of sound in the inviscid flow, the waves well within the boundary layer are propagating at a speed on the order of the freestream velocity and thus the boundary layer is being excited by the classical Tollmein Schlichting waves. The analysis thus indicates that the effect of acoustical disturbances on transition is similar to the effect of other perturbations as experiments have indicated.

ACKNOWLEDGEMENT

This technical report covers the work performed under Contract N00014-76-C-1083 from 15 September 1975 to 15 December 1977 and is the annual report for this period. The program is sponsored by the Office of Naval Research.

TABLE OF CONTENTS

I. INTRODUCTION

In recent years several investigators (for example, Refs. 1 and 2) have developed numerical analyses to investigate the nonlinear effects of disturbances propagating in a laminar boundary layer with a view towards a better understanding of boundary layer stability. Such investigations are extensions of earlier linear stability analyses (for example, Refs. 3-7) and were motivated by the work of Stuart[8] and others who viewed the transition process as a series of distinctly observable stages. In the first stage, the two dimensional Tollmien-Schlichting waves are developed and the flowfield can be analyzed linearly. However, downstream of this region, nonlinear and three dimensional effects begin to play a more and more dominant role. Thus a complete physical understanding of the transition phenomenon must await the development of a nonlinear, three dimensional program capable of measuring amplification of the waves as they propagate.

Numerical analyses capable of solving the nonlinear system of equations in the boundary layer (even two dimensional codes) can be extremely useful for the study of the wave amplification phenomenon. Linear stability theory, exemplified by eigen solutions of the Orr-Summerfeld equations, cannot directly incorporate the properties of imposed disturbances. Once disturbances are introduced, the mechanism of introduction not appearing in these solutions, it is presumed that they can no longer significantly influence the boundary layer process, which is, perhaps, a serious shortcoming of linear theory.

Nonlinear analyses (such as Refs. 1 and 2) have investigated the stability of laminar, incompressible boundary layers and the initial phase of the transition process (prior to the three dimensional bursting phase) by direct numerical solution of the partial differential equations which describe such a process. The boundary layer flow on a flat plate is disturbed by forced time-dependent perturbations, and the reaction of the flow, i.e. the temporal and spatial development of the perturbations, is determined by a numerical solution of the governing equations. Such programs thus have the ability to analyze the effects of large scale disturbances (i.e. on the order of .1% of the free stream velocity) and how they are amplified or damped by the boundary layer, whereas linear stability programs cannot directly incorporate the effect of disturbance amplitude into the stability calculation.

While these nonlinear analyses represent a significant advance in the state of the art, they are restricted to incompressible flow. The effects of such parameters as Mach number and wall temperature are, of course, of great significance and a compressible analog to these methods is necessary.

In addition, such programs are unable to determine directly the effects of imposed acoustical disturbances. Experiments, for example Refs. 9 and 10, have indicated that the effects of imposed acoustic perturbations on boundary layer transition is similar to the effects of freestream turbulence[11] in low speed flow. One would expect waves propagating through the flowfield at the speed of sound to affect boundary layer transition in a different way than waves propagating through at the freestream velocity, but the Spangler and Wells experiments, as well as others, have shown that this is not the case. The frequency range which affects transition at a given Reynolds number is the same as when freestream disturbances are introduced, even though there appears to be a mismatch in propagation velocity (and thus in wave number).

The necessity for a study of the effects of these acoustical disturbances was the motivation of the present investigation and it's extension. The unsteady, compressible,second order boundary layer equations have been utilized. Terms of the order of the reciprocal of the Reynolds number and the reciprocal squared have been retained and thus the system is consistent with the Navier Stokes equations. These equations have been solved by an explicit scheme in the high Reynolds number range (where the equations are, essentially, the boundary layer equations) consistent with the experiments of Spangler and Wells.

In Section II, the equations of motion and, method of analysis is developed. In Section III, the results and conclusions of the present investigation are presented. This work is part of a continuing effort and additional results, especially with regards to the effects of such parameters as Mach number and wall temperature, will be forthcoming.

II. METHOD OF ANALYSIS

A. Equations of Motion

The system of equations have have been utilized are the compressible, two-dimensional, higher order boundary layer equations (retaining terms of order $1/Re$ and $1/Re^2$). This system is thus, essentially, the compressible Navier Stokes equations. For unit Prandtl number, the system, for a perfect gas is;

$$\frac{\partial \bar{\rho}}{\partial \bar{t}} + \frac{\partial}{\partial \bar{x}}(\bar{\rho}\bar{u}) + \frac{\partial}{\partial \bar{y}}(\bar{\rho}\bar{v}) = 0 \tag{1}$$

$$\frac{\partial}{\partial \bar{t}}(\bar{\rho}\bar{u}) + \frac{\partial}{\partial \bar{x}}(\bar{\rho}\bar{u}^2 + \bar{p}) + \frac{\partial}{\partial \bar{y}}(\bar{\rho}\bar{u}\bar{v}) = \frac{\partial}{\partial \bar{y}}\left[\bar{\mu}\frac{\partial \bar{u}}{\partial \bar{y}}\right] + \phi_1$$

$$\frac{\partial}{\partial \bar{t}}(\bar{\rho}\bar{v}) + \frac{\partial}{\partial \bar{x}}(\bar{\rho}\bar{u}\bar{v}) + \frac{\partial}{\partial \bar{y}}\left[\bar{\rho}\bar{v}^2 + Re_L \cdot \bar{p}\right] = \frac{4}{3}\frac{\partial}{\partial \bar{y}}\left[\bar{\mu}\frac{\partial \bar{v}}{\partial \bar{y}}\right] \tag{2}$$

$$-\frac{2}{3}\frac{\partial}{\partial \bar{y}}\left(\bar{\mu}\frac{\partial \bar{u}}{\partial \bar{x}}\right) + \frac{\partial}{\partial \bar{x}}\left(\bar{\mu}\frac{\partial \bar{u}}{\partial \bar{y}}\right) + \phi_2 \tag{3}$$

$$\frac{\partial}{\partial \bar{t}}(\bar{\rho}\bar{E}) + \frac{\partial}{\partial \bar{x}}(\bar{\rho}\bar{u}\bar{H}) + \frac{\partial}{\partial \bar{y}}(\bar{\rho}\bar{v}\bar{H}) = \frac{\partial}{\partial \bar{y}}\left[\bar{\mu}\frac{\partial \bar{H}}{\partial \bar{y}}\right] + \phi_3 \tag{4}$$

$$\bar{p} = \bar{\rho}\bar{T} \tag{5}$$

where

$$\bar{x} = \frac{x}{L}; \quad \bar{y} = \frac{y}{L}\cdot\sqrt{Re_L}; \quad \bar{t} = t\,\frac{u_\infty}{L}$$

$$\bar{u} = \frac{u}{u_\infty}; \quad \bar{v} = \frac{v}{u_\infty}\cdot\sqrt{Re_L}; \quad \bar{p} = \frac{p}{\rho_\infty u_\infty^2}; \quad \bar{\rho} = \frac{\rho}{\rho_\infty}$$

$$\bar{H} = \frac{H}{u_\infty^2} = \frac{C_p T}{u_\infty^2} + \frac{u^2 + v^2}{2u_\infty^2}; \quad \bar{E} = \frac{E}{u_\infty^2} = \frac{C_v T}{u_\infty^2} + \frac{u^2 + v^2}{2u_\infty^2}$$

$$\bar{\mu} = \frac{\mu}{\mu_\infty} = \frac{T_\infty + 198.6}{T + 198.6}\left(\frac{T}{T_\infty}\right)^{3/2}; \quad \bar{T} = \frac{RT}{u_\infty^2} \qquad Re_L = \frac{\rho_\infty u_\infty L}{\mu_\infty}$$

$$\phi_1 = \frac{1}{Re_L}\left[\frac{4}{3}\frac{\partial}{\partial \bar{x}}\left(\bar{\mu}\frac{\partial \bar{u}}{\partial \bar{x}}\right) - \frac{2}{3}\frac{\partial}{\partial \bar{x}}\left(\bar{\mu}\frac{\partial \bar{v}}{\partial \bar{y}}\right) + \frac{\partial}{\partial \bar{y}}\left(\bar{\mu}\frac{\partial \bar{v}}{\partial \bar{x}}\right)\right]$$

$$\phi_2 = \frac{1}{Re_L}\frac{\partial}{\partial \bar{x}}\left(\bar{\mu}\frac{\partial v}{\partial \bar{x}}\right)$$

$$\phi_3 = \frac{1}{Re_L}\left[\frac{\partial}{\partial \bar{x}}\left(\bar{\mu}\frac{\partial \bar{H}}{\partial \bar{x}}\right) + \frac{1}{3}\bar{\mu}\left(\frac{\partial \bar{u}}{\partial \bar{x}}\right)^2 + \frac{1}{3}\bar{\mu}\left(\frac{\partial \bar{v}}{\partial \bar{y}}\right)^2 - \frac{2}{3}\bar{\mu}\frac{\partial \bar{u}}{\partial \bar{x}}\frac{\partial \bar{v}}{\partial \bar{y}} + 2\bar{\mu}\frac{\partial \bar{v}}{\partial \bar{x}}\frac{\partial \bar{u}}{\partial \bar{y}}\right.$$

$$- \frac{1}{2}\frac{\partial \bar{\mu}}{\partial \bar{x}}\frac{\partial}{\partial \bar{x}}(\bar{u}^2) - \frac{1}{2}\frac{\partial \bar{\mu}}{\partial \bar{x}}\frac{\partial \bar{v}^2}{\partial \bar{x}}\frac{1}{Re_L} - \frac{1}{2}\frac{\partial \bar{\mu}}{\partial \bar{y}}\frac{\partial \bar{v}^2}{\partial \bar{y}}\Big]$$

$$- \frac{1}{2}\frac{\partial \bar{\mu}}{\partial \bar{y}}\frac{\partial \bar{u}^2}{\partial \bar{y}}$$

In order to study the effect of the propagation of acoustical free-stream disturbances, the equations have been transformed by a stretched coordinate system which packs many points into the boundary layer, but allows for a significant distribution of data in the freestream. The transformation utilized is:

$$\eta = 1 - \exp(-\alpha\bar{y}/\bar{\delta}^*) \tag{6}$$

where $\bar{\delta}^* = \delta_0^*/L \sqrt{Re_L}$ and $\delta_0^*(x)$ is the initial boundary layer displacement thickness distribution (i.e., the distribution at $\bar{t} = 0$). Thus by varying α one can pack as many points as needed near the surface (note as $\bar{y} \to \infty, \eta \to 1$).

The system of equations in the transformed system is;

$$\frac{\partial \bar{\rho}}{\partial \bar{t}} + \frac{\partial}{\partial \bar{x}}(\bar{\rho}\bar{u}) + \frac{\partial}{\partial \eta}(\bar{\rho}\bar{u})\frac{\partial \eta}{\partial \bar{x}} + (1-\eta)\frac{\alpha}{\bar{\delta}^*}\frac{\partial \bar{\rho}\bar{v}}{\partial \eta} = 0 \tag{7}$$

$$\frac{\partial}{\partial \bar{t}}(\bar{\rho}\bar{u}) + \frac{\partial}{\partial \bar{x}}(\bar{\rho}\bar{u}^2 + \bar{p}) + \frac{\partial}{\partial \eta}(\bar{\rho}\bar{u}^2 + \bar{p})\frac{\partial \eta}{\partial \bar{x}} + (1-\eta)\frac{\alpha}{\bar{\delta}^*}\frac{\partial}{\partial \eta}(\bar{\rho}\bar{\mu}\bar{v})$$

$$= \frac{\alpha^2(1-\eta)}{\bar{\delta}^{*2}}\frac{\partial}{\partial \eta}\left[\bar{\mu}(1-\eta)\frac{\partial \bar{u}}{\partial \eta}\right] + \phi_4 \tag{8}$$

$$\frac{\partial}{\partial \bar t}(\bar\rho\bar v) + \frac{\partial}{\partial \bar x}(\bar\rho\bar u\bar v) + \frac{\partial}{\partial \eta}(\bar\rho\bar u\bar v)\frac{\partial\eta}{\partial\bar x} - (1-\eta)\frac{\alpha}{\bar\delta^*}\frac{\partial}{\partial\eta}(\bar\rho\bar v^2 + \bar p\ Re_L) \tag{9}$$

$$= \frac{4}{3}\frac{\alpha^2}{\bar\delta^{*2}}(1-\eta)\frac{\partial}{\partial\eta}[\bar\mu(1-\eta)\frac{\partial\bar v}{\partial\eta}] - \frac{2}{3}(1-\eta)\frac{\alpha}{\bar\delta^*}\frac{\partial}{\partial\eta}[\bar\mu\frac{\partial\bar u}{\partial\bar x} + \bar\mu\frac{\partial\eta}{\partial\bar x}\frac{\partial\bar u}{\partial\eta}]$$

$$+ \frac{\partial}{\partial\bar x}[\bar\mu(1-\eta)\frac{\alpha}{\bar\delta^*}\frac{\partial\bar u}{\partial\eta}] + \frac{\partial\eta}{\partial\bar x}\frac{\partial}{\partial\eta}[\bar\mu(1-\eta)\frac{\alpha}{\bar\delta^*}\frac{\partial\bar u}{\partial\eta}] + \phi_5$$

$$\frac{\partial}{\partial t}(\bar\rho\bar E) + \frac{\partial}{\partial\bar x}(\bar\rho\bar u\bar H) + \frac{\partial}{\partial\eta}(\bar\rho\bar u\bar H)\frac{\partial\eta}{\partial\bar x} + (1-\eta)\frac{\alpha}{\bar\delta^*}\frac{\partial}{\partial\eta}(\bar\rho\bar u\bar H) \tag{10}$$

$$= \frac{\alpha^2(1-\eta)}{\bar\delta^{*2}}\frac{\partial}{\partial\eta}[\bar\mu(1-\eta)\frac{\partial\bar H}{\partial\eta}] + \phi_6$$

$$\bar p = \bar\rho\bar T \tag{11}$$

where

$$\phi_4 = \frac{1}{Re_L}\{\frac{4}{3}\frac{\partial}{\partial\bar x}(\bar\mu\frac{\partial\bar u}{\partial\bar x}) - \frac{2}{3}\frac{\alpha}{\bar\delta^*}\frac{\partial}{\partial\bar x}[\bar\mu(1-\eta)\frac{\partial\bar v}{\partial\eta}]$$

$$+ \frac{4}{3}\frac{\partial\eta}{\partial\bar x}\frac{\partial}{\partial\eta}(\bar\mu\frac{\partial\bar u}{\partial\bar x}) - \frac{2}{3}\frac{\alpha}{\bar\delta^*}\frac{\partial\eta}{\partial\bar x}\frac{\partial}{\partial\eta}[\bar\mu(1-\eta)\frac{\partial\bar v}{\partial\eta}]$$

$$+ (1-\eta)\frac{\alpha}{\bar\delta^*}\frac{\partial}{\partial\eta}(\bar\mu\frac{\partial\bar v}{\partial\bar x})$$

$$+ \frac{4}{3}\frac{\partial}{\partial\bar x}(\bar\mu\frac{\partial\eta}{\partial\bar x}\frac{\partial\bar u}{\partial\eta}) + \frac{4}{3}\frac{\partial\eta}{\partial\bar x}\frac{\partial}{\partial\eta}(\bar\mu\frac{\partial\eta}{\partial\bar x}\frac{\partial\bar u}{\partial\eta})$$

$$+ \frac{\alpha}{\bar\delta^*}(1-\eta)\frac{\partial}{\partial\eta}(\bar\mu\frac{\partial\eta}{\partial\bar x}\frac{\partial\bar v}{\partial\eta})\}$$

$$\phi_5 = \frac{1}{Re_L}[\frac{\partial}{\partial\bar x}(\bar\mu\frac{\partial\bar v}{\partial\bar x}) + \frac{\partial\eta}{\partial\bar x}\frac{\partial}{\partial\eta}(\bar\mu\frac{\partial\bar v}{\partial\bar x})$$

$$+ \frac{\partial}{\partial\bar x}(\frac{\partial\eta}{\partial\bar x}\frac{\partial\bar v}{\partial\eta}) + (\frac{\partial\eta}{\partial\bar x})\frac{\partial}{\partial\eta}(\frac{\partial\eta}{\partial\bar x}\frac{\partial\bar v}{\partial\eta})]$$

$$\phi_6 = \frac{1}{Re_L}\{[\frac{\partial}{\partial\bar x} + \frac{\partial\eta}{\partial\bar x}\frac{\partial}{\partial\eta}][\bar\mu\frac{\partial\bar H}{\partial\bar x} + \frac{\partial\eta}{\partial\bar x}\frac{\partial\bar H}{\partial\eta}]$$

$$+ \frac{1}{3}\bar\mu(\frac{\partial\bar u}{\partial\bar x} + \frac{\partial\eta}{\partial\bar x}\frac{\partial\bar u}{\partial\eta})^2 + \frac{1}{3}\bar\mu(\frac{\partial\bar v}{\partial\bar x} + \frac{\partial\eta}{\partial\bar x}\frac{\partial\bar v}{\partial\eta})^2$$

$$- \frac{2}{3}\frac{\alpha(1-\eta)}{\bar\delta^*}\bar\mu(\frac{\partial\bar u}{\partial\bar x} + \frac{\partial\eta}{\partial\bar x}\frac{\partial\bar u}{\partial\eta})\frac{\partial\bar v}{\partial\eta}$$

$$+ \frac{2\alpha(1-\eta)}{\bar\delta^*}\bar\mu(\frac{\partial\bar v}{\partial\bar x} + \frac{\partial\eta}{\partial\bar x}\frac{\partial\bar v}{\partial\eta})\frac{\partial\bar u}{\partial\eta}$$

$$- \frac{1}{2}(\frac{\partial\bar\mu}{\partial\bar x} + \frac{\partial\eta}{\partial\bar x}\frac{\partial\bar\mu}{\partial\eta})(\frac{\partial(\bar u^2)}{\partial\bar x} + \frac{\partial\eta}{\partial\bar x}\frac{\partial\bar u^2}{\partial\eta})$$

$$- \frac{1}{2Re_L} \left(\frac{\partial \bar{u}}{\partial \bar{x}} + \frac{\partial \eta}{\partial \bar{x}} \frac{\partial \bar{u}}{\partial \eta} \right) \left(\frac{\partial \bar{v}^2}{\partial \bar{x}} + \frac{\partial \eta}{\partial \bar{x}} \frac{\partial \bar{v}^2}{\partial \eta} \right)$$

$$- \frac{1}{2} \frac{\alpha^2}{\bar{\delta}^{*2}} (1 - \eta)^2 \frac{\partial \bar{v}^2}{\partial \eta} \}$$

$$- \frac{\alpha^2}{\bar{\delta}^{*2}} (1 - \eta)^2 \frac{\partial \bar{u}}{\partial \eta} \frac{\partial \bar{u}^2}{\partial \eta}$$

Equations (7) through (11) are the basic system of equations which have been numerically solved.

B. Initial and Boundary Conditions

The investigation has centered on a study of the amplification or damping of acoustical disturbances propagated into a boundary layer. The experiments of Spangler and Wells[9] who utilized an air-driven, rotating vane sound generator to create the disturbance without producing any appreciable turbulence, were used. Both the frequency and intensity of the sound source were varied experimentally. A low velocity boundary layer channel was run at a unit Reynolds number of 2.4×10^5/ft., the channel wall representing the flat plate. Measurements of transition occurred at distances on the order of 10-20 feet, and thus the length Reynolds numbers of interest are in the 10^6 to 10^7 range (see next section).

In order to model this problem, a set of initial and boundary conditions must be established, consistent with the propagation of acoustical disturbances and at the same time consistent with the set of differential equations utilized. The initial data, consistent with equations (1) through (5) under steady state conditions, was originally established utilizing numerical techniques for subsonic boundary layer analysis with normal pressure gradients established by the principal investigator and reported previously, i.e., Ref. 12. Thus the solution at $\bar{t}$ = o was the solution of the two dimensional steady boundary layer equations with normal momentum equation included.

During the past year, consistent with Refs. 1 and 2, the Blasius solution has been utilized (since for the cases of interest, $M_\infty \approx .03$) and has caused no major problems.

At the wall (η = o), for a rigid body, one can neglect the effect of the wave on temperature, and for an adiabatic wall one can establish the following relations (if one drops terms of order 1/Re which implies some inconsistency for lower Re)

$$\eta = 0 \ (\bar{x} > \bar{x}^*)$$

$$\bar{u} = \bar{v} = \frac{\partial \bar{T}}{\partial \eta} = 0$$

$$\frac{\partial}{\partial \eta}(\ell n \bar{p}) = \frac{\partial}{\partial \eta}[(\ell n \bar{p})]_{\bar{t}=0} \exp\left[-Re_L \int_0^{\bar{t}} \frac{\bar{p}}{\bar{\mu}} d\bar{t}\right]$$

$$\frac{\partial}{\partial \eta}(\ell n \bar{\rho}) = \frac{\partial}{\partial \eta}[(\ell n \bar{\rho})]_{\bar{t}=0} \exp\left[-Re_L \int_0^{t} \frac{\bar{p}}{\bar{\mu}} d\bar{t}\right]$$

The outer boundary condition ($\eta \to 1$) is established by allowing the wave to travel as a plane wave with speed of sound c_∞.

Much effort has been placed on the determination of a proper downstream boundary condition. It has been found, consistent with the results of Fasel[1], that the boundary condition that yields the least upstream influence, and is thus superior to other possible ones (including a non reflective condition) is:

$$\frac{\partial^2 \bar{u}'(\bar{x}_f, \bar{y}, \bar{t})}{\partial \bar{x}^2} = \bar{\alpha}^2 \bar{u}'$$

where $\bar{\alpha} = fL/V_{ph}$ (f is the frequency and V_{ph} the phase velocity), $\bar{u}'$ is the perturbation quantity ($\bar{u} - \bar{u}_0$), and $\bar{x}_f$ is the downstream boundary. This condition says that at the downstream boundary, the disturbance has a periodic form.

At $\bar{t} = o$, an acoustical disturbance is initiated at $\bar{x} \approx o$ so that the velocity field at $x = x^* \approx o$ and $\bar{t} > o$ can be written as

$$\bar{u}(\bar{x}^*, \bar{y}, \bar{t}) = \bar{u}_o(\bar{x}^*, \bar{y}) + f_1(\bar{y}) \sin(\bar{\omega}\bar{t})$$

where $\bar{u}_o(\bar{x}^*, \bar{y})$ is the velocity profile at $\bar{t} = o$, $\bar{\omega} = 2\pi fL/U_\infty$ (f being the frequency of the imposed disturbance, in cycles per second) and $f_1(\bar{y})$ is the disturbance profile near the leading edge. The form of $f_1(\bar{y})$ has been the object of extensive analysis and is described here. The other boundary conditions at $x = x^*$ are consistent with linear theory and are determined once the form of $f_1(\bar{y})$ is known.

In order to derive appropriate perturbation profiles for use as the initial boundary condition in our program (at $\bar{x} = \bar{x}^*$) the compressible analogue of the Orr-Sommerfeld equations must be solved. We have at present considered these equations in the inviscid limit and under the additional assumption of no temperature gradient in the mean flow.

Thus nondimensionalizing all lengths by the boundary layer thickness δ at a suitable station along the plate, all velocities by the free stream speed of sound, and the pressure by $\rho_\infty c_\infty^2$, the linearized perturbation system solved is;

$$i(ku_o - \omega)\rho + iku\rho_o + \frac{d}{dy}(\rho_o V) = 0 \tag{12}$$

$$i(ku_o - \omega)u + u_o' V + \frac{ik}{\rho_o} p = o \tag{13}$$

$$i(ku_o - \omega)V + \frac{1}{\rho_o}\frac{dp}{dy} = o \tag{14}$$

$$i(ku_o - \omega)T + T_o' V = i\left(\frac{\gamma - 1}{\rho_o}\right)(ku_o - \omega)p \tag{15}$$

$$p/p_o = \rho/\rho_o + T/T_o \tag{16}$$

where bars have been dropped and subscript zero refers to the profile at $t = o$. The appropriate boundary conditions are discussed below. As is customary the normal mode decomposition has been used, and hence we note that ρ, u, V, p, T are functions of y, the distance normal to the plate. The parameters ω and k, the dimensionless frequency and wave number respectively are given by

$$\omega = \Omega\delta/_{c_\infty}, \; k = \bar{k}\delta$$

where Ω and $\bar{k}$ are dimensional quantities. The mean flow quantities

$$u_o = M_\infty u_B \text{ and } u_o' = 5.6 \; (M_\infty \frac{du_B}{d\eta})$$

are the dimensionless velocity and velocity gradient respectively where M_∞ is the freestream Mach number, u_B is the dimensionless Blasius profile and the factor 5.6 results from changing the normal coordinate from η to y.

Several simplifications can be made in equations (12 - 16). We have solved for ρ, u, v and T in terms of the pressure p and find that p must satisfy the second order equation

$$p'' - \frac{2ku_o'}{u_o k-\omega} p' + [\frac{(u_o k - \omega)^2}{T_o} - k^2] p = o \qquad (17)$$

In solving this equation we have considered ω as fixed and k as an unknown to be found. (In general, the phase velocity, $V_p = \omega/k$ and the wave number can be complex). For the present we are considering neutral stability and thus k and V_p are real, however, we plan to extend the calculation to include complex k.

To derive suitable boundary conditions, we assume that at the plate the perturbation V, in the normal velocity is zero and since

$$V = \frac{i}{\rho_o(ku_o - \omega)} \frac{dP}{dy}$$

we take

$$\frac{dP}{dy} = o \text{ at } y = o.$$

To derive a boundary condition at the top of the boundary layer or in the free stream, we write equation (17) in the free stream, i.e. with $u_o' = o$ and $u_B = 1$. Then the equation has constant coefficients and can be readily solved. The nature of the solutions, depends of course, on the sign of $\lambda = -(M_\infty k - \omega)^2 + k^2$.

For the frequency and Mach numbers considered, λ is positive and hence $p = C_1 \exp(-\sqrt{\lambda} y)$ is the solution of (17) which vanishes at infinite distances from the plate. Using this solution to provide boundary conditions for the top of the boundary layer we have

$$\frac{dp(1)}{dy} = -\sqrt{\lambda} = -\sqrt{k^2 - (M_\infty k - \omega)^2} \quad \text{and } p(1) = 1 \qquad (18)$$

We note that the second condition is a normalization condition.

Equations (12) - (17) now provide an eigenvalue problem for the eigenvalue k. Once k is determined, the profiles at $x = \bar{x}^*$ (i.e. the $f_1(y)$) can be determined and thus the initial and boundary conditions for the calculation are entirely prescribed.

C. Numerical Method

The MacCormack predictor corrector scheme has been utilized in the study. Equations (7) - (10) are four equations of the form

$$\frac{\partial e}{\partial t} = a_1 \frac{\partial f}{\partial x} + a_2 \frac{\partial g}{\partial \eta} + a_3 \frac{\partial^2 h}{\partial \eta^2} + a_4 \frac{\partial^2 i}{\partial \bar{x}^2} + a_5 \frac{\partial^2 j}{\partial \bar{x} \partial \eta}$$

If these equations are written as

$$\frac{\partial e_i}{\partial t} (\bar{x}, \eta, \bar{t}) = F(\bar{x}, \eta, \bar{t})$$

$$e_1 = \bar{\rho}, \quad e_2 = \bar{\rho}\bar{u}, \quad e_3 = \bar{\rho}\bar{v}, \quad e_4 = \bar{\rho}\bar{E}$$

the MacCormack method states that

$$e(\bar{x}, \eta, \bar{t} + \bar{\Delta}t) = e(\bar{x}, \eta, \bar{t}) + 1/2[F(\bar{x}, \eta, \bar{t}) + F(\bar{x}, \eta, \bar{t} + \bar{\Delta}t)]\Delta\bar{t}$$

In order to solve for $e\,(\bar{x}, \eta, \bar{t} + \Delta\bar{t})$ one first calculates a provisional solution,

$$e^{(1)}(\bar{x},\eta, \bar{t} + \Delta\bar{t}) = e(\bar{x}, \eta, \bar{t}) + F^{(+)}(\bar{x}, \eta, \bar{t})\, \Delta\bar{t}$$

where $F^{(+)}$ refers to evaluation by non-centered differences, using values at $\bar{x} + \Delta\bar{x}$, $\eta + \Delta\eta$, $\bar{x}$, and η, e. g.

$$\frac{\partial f}{\partial x} = \frac{f(\bar{x} + \Delta\bar{x}, \eta, \bar{t}) - f(\bar{x}, \eta, \bar{t})}{\Delta\bar{x}}$$

then one can use $e^{(1)}$ to evaluate the term $F^{(-)}(\bar{x}, \eta, \bar{t} + \Delta\bar{t})$ using non-centered differences based on $\bar{x} - \Delta\bar{x}$, $\eta - \Delta\eta$, $\bar{x}$, η; e.g.,

$$\frac{\partial f}{\partial x} = \frac{f^{(-)}(\bar{x}, \eta, \bar{t} + \Delta\bar{t}) - f^{(-)}(\bar{x} - \Delta\bar{x}\ \eta, \bar{t} + \Delta\bar{t})}{\Delta\bar{x}}$$

Thus one can solve for $e\,(\bar{x}, \eta, \bar{t} + \Delta\bar{t})$ from the system,

$$e\,(\bar{x}, \eta, \bar{t} + \Delta\bar{t}) = 1/2[e\,(\bar{x}, \eta, \bar{t}) + e^{(1)}(\bar{x}, \eta, \bar{t} + \Delta\bar{t})$$
$$+ F^{(-)}(\bar{x}, \eta, \bar{t} + \Delta\bar{t})\ \Delta\bar{t}]$$

Equations (7) - (10), the full unsteady compressible Navier Stokes system are a complex set of elliptic differential equations to numerically integrate. No other nonlinear analysis, that we are aware of, has attempted to solve the compressible system for the present application (both Fasel and Murdock solve the incompressible problem). The explicit MacCormack scheme was seen as a simpler method for the solution of this system as opposed to an implicit (or ADI) method.

The problem with utilizing an explicit scheme for such calculations is manifested in the problem of the time step which can be utilized in order to insure a stable solution. Since $\Delta y << \Delta x$ in the boundary layer, the time step to satisfy the C.F.L. condition is such that $\Delta t < \Delta y/c$, which is extremely small, and in order to insure on the order of ten time periods for the frequencies of interest, on the order of 10^5 time steps would be required. We have noticed though that for the problems of interest (the modeling of the experiments of Ref. 8) the local Reynolds numbers of interest are greater than 10^6 and thus the leading terms are the parabolic system (i.e., the first order boundary layer equations). The parabolic system has a much less stringent time size criteria (like $\Delta t < \Delta y^2/2\nu$).

For the grid sizes used in the present investigation, $\Delta\bar{t} \sim M_\infty \Delta\bar{x}$ satisfies the parabolic time step criteria ($\Delta\bar{t} < \Delta\bar{y}^2/2$). Over the time scale of interest (on the order of ten perturbation periods) the relaxation of the C.F.L. criteria is manifested not in a gross instability (because of the very high Reynolds numbers) but as a drift in the solution. This was noticed by imposing a zero perturbation field at the station $\bar{x} = \bar{x}^*$ (i.e., $f_1(y) = o$) and tracking the perturbation solution ($\bar{u} - \bar{u}_{Blasius}$). The program was thus modified to circumvent this problem in the following manner. At any time step, the equations are solved under two sets of conditions, first for the flow without external disturbance (i.e., $f_1(y) = o$) and then for the flow with disturbance. The solution of every point at each time step is then taken as the difference between the two solutions. Thus it is felt that any errors due to numerics have been suppressed. The time traces which will be presented in the next section exhibit no drift and, thus, we feel that the oscillations at each position in the flowfield are due only to the disturbance imposed and are not numerical in nature. At lower Reynolds numbers or for times greater than those of the present calculations the error introduced by not satisfying the C.F.L. will grow and an instability will undoubtedly occur, necessitating one to resort to time splitting (or some other such technique). During the coming year, the program will be modified towards this end.

IV. THE PRESENT INVESTIGATION AND RESULTS TO DATE

One of the tasks that was pursued this year was an attempt to interpret the results of experimental investigations of large scale (.1% to 1% of freestream) perturbations on boundary layer stability. The experimental results of Klebanoff and Tidstrom [14] for boundary layer transition induced by a two dimensional roughness element were examined in detail towards this end.

Figure 1 (reproduced from Reference 14) presents the longtitudinal velocity fluctuations downstream of the roughness element. In the top figure, the fluctuations directly downstream of the element (located at $x = x_k = 2$ ft) for a unit Reynolds number of 1.16×10^5/ft are plotted as a function of frequency. At the end of the recovery zone ($x - x_k \approx 4.5$ in) amplification in the Tollmien Schlichting range has occurred. In the lower figure the transverse profiles, for a range of unit Reynolds numbers are presented. At larger unit Reynolds numbers, transition occurred in the recovery zone and the analysis presented below is no longer pertinent. For the unit Reynolds number 1.16×10^5/ft the boundary layer profile became highly inflected (and more unstable) downstream of the element until $x - x_k = 4.5$ in where the profile returns to a Blasius representation, as is shown in Figure 2 taken from Reference 14. For this case, transition occurs at $x - x_k = 19$ in.

Thus for a length of approximately two feet, a Blasius like flowfield is under the influence of a large perturbation ($U'/U_\infty > .1\%$ at $x - x_k = 4.5$ in) initial profile. This initial profile is shown by the triangles in (b) of the lower figure of Figure 1. This profile corresponds to a linear spatial stability profile for 50 cycles/sec (the dominant mode for the case) but for a somewhat higher Reynolds number (the roughness element has, of course, amplified the

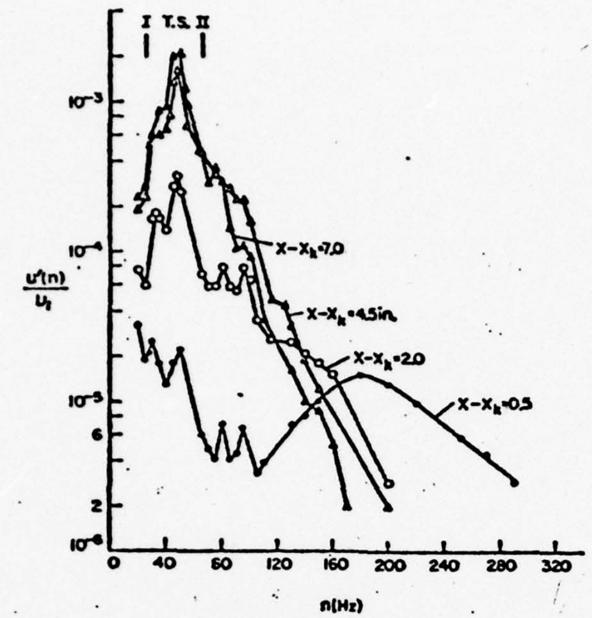

Spectra of u fluctuation downstream of 0.066-in. diam roughness element at x_k=2.0 ft, U_e/ν=1.16×10^5 (ft^{-1}), y=0.06 in.

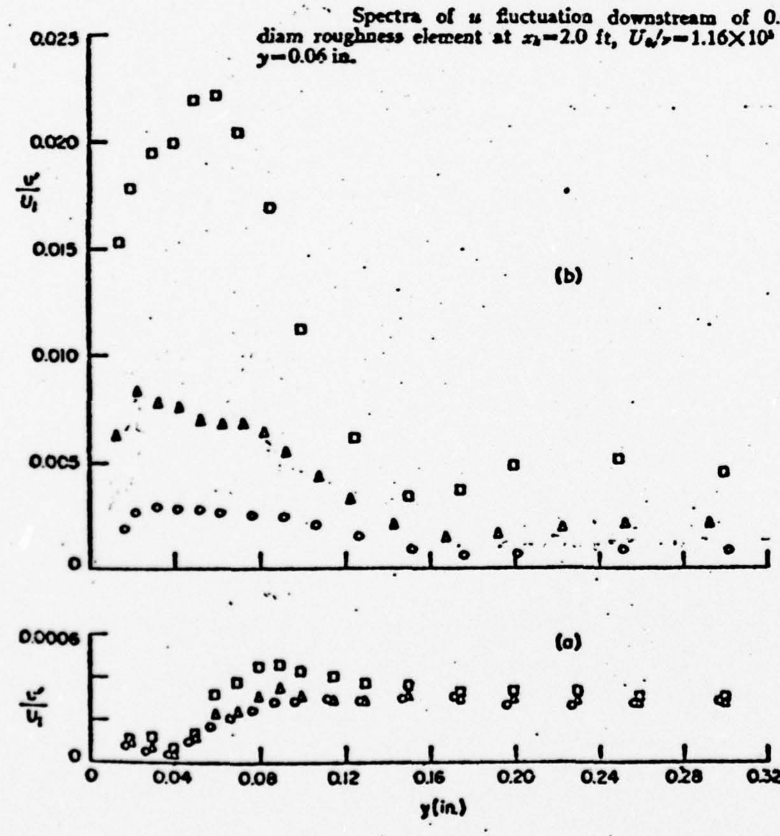

Intensity of u fluctuation downstream of 0.066-in. diam roughness element at x_k=2.0 ft, illustrating increase in amplification within recovery zone. ⊙ U_e/ν=1.0×10^5 (ft^{-1}), △ U_e/ν=1.16×10^5 (ft^{-1}), ⊡ U_e/ν=1.42×10^5 (ft^{-1}). (a) $x-x_k$=0.5 in. (b) $x-x_k$=4.5 in.

FIGURE 1. LONGITUDINAL VELOCITY FLUCTUATIONS DOWNSTREAM OF ROUGHNESS ELEMENT

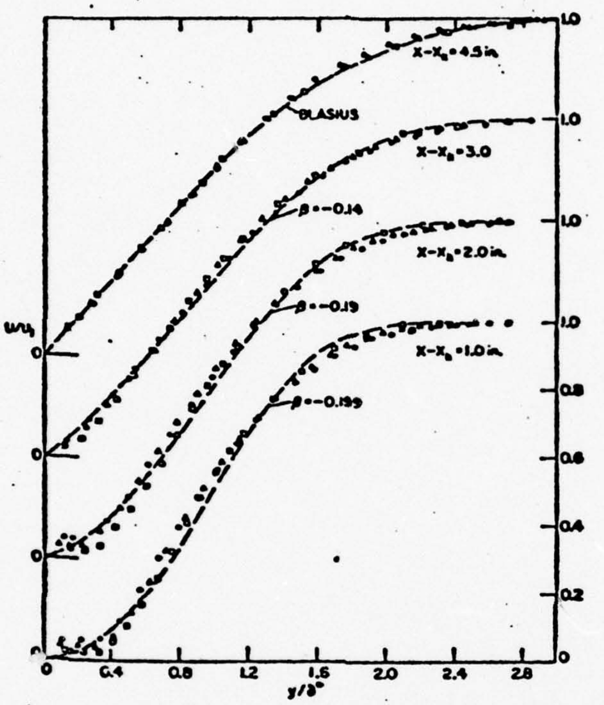

Mean-velocity distributions downstream of 0.066-in. diam roughness element at $x_k = 2.0$ ft compared with Hartree profiles; ⊙ $U_e/\nu = 1.0 \times 10^5$ (ft^{-1}); △ $U_e/\nu = 1.16 \times 10^5$ (ft^{-1}); ⊡ $U_e/\nu = 1.42 \times 10^5$ (ft^{-1}).

FIGURE 2. MEAN PROFILES IN RECOVERY ZONE

the boundary layer response at this station). Therefore, downstream of $x - x_k = 4.5$ in, the boundary layer is acting like a typical flat plate boundary layer under the influence of a large initial disturbance profile. We will attempt to show similarities between this flowfield (or the forced response to other larger scale perturbations) and the response to acoustical disturbances, by an examination of the results of our computer code.

For the computation of the acoustic response, one must first solve the linear acoustic stability problem (at $\bar{x} = \bar{x}^*$) as described in the previous section. Such analyses have been performed. An eigenvalue search indicates that for a given frequency, the wave numbers corresponding to the eigen solutions occur at propagation velocities on the order of the freestream velocity (actually two to three times larger). Thus the results of Refs. 5 and 6 are correct, even for an acoustical disturbance, in the linear range.

The computer program for the solutions of equations (7) - (10) has been run for certain cases corresponding to the Reynolds number and frequency range of the Spangler and Wells experiments. Figure 3 presents the results of three such computations for the forced response of the boundary layer to acoustic waves of different frequencies (using linear stability theory at $\bar{x}^* = .025$). For these cases the values of $U'_{R.M.S.}$ taken was .3% of the freestream.

Linear stability theory would predict that for the length Reynolds number of interest for the Spangler and Wells experiments ($\approx 3 \times 10^6$ at x = 12 ft) a frequency of 27 cycles/sec is within the unstable region, whereas at 150 cycles/sec the flow is stable. This factor is evident in Figure 3. The 43 cycles/sec case exhibits neither amplification or damping (and thus appears neutrally stable) a factor which does not agree with the experimental results which show early transition at 43 cycles. It may be possible that if the computation were carried further in time some amplification would exist.

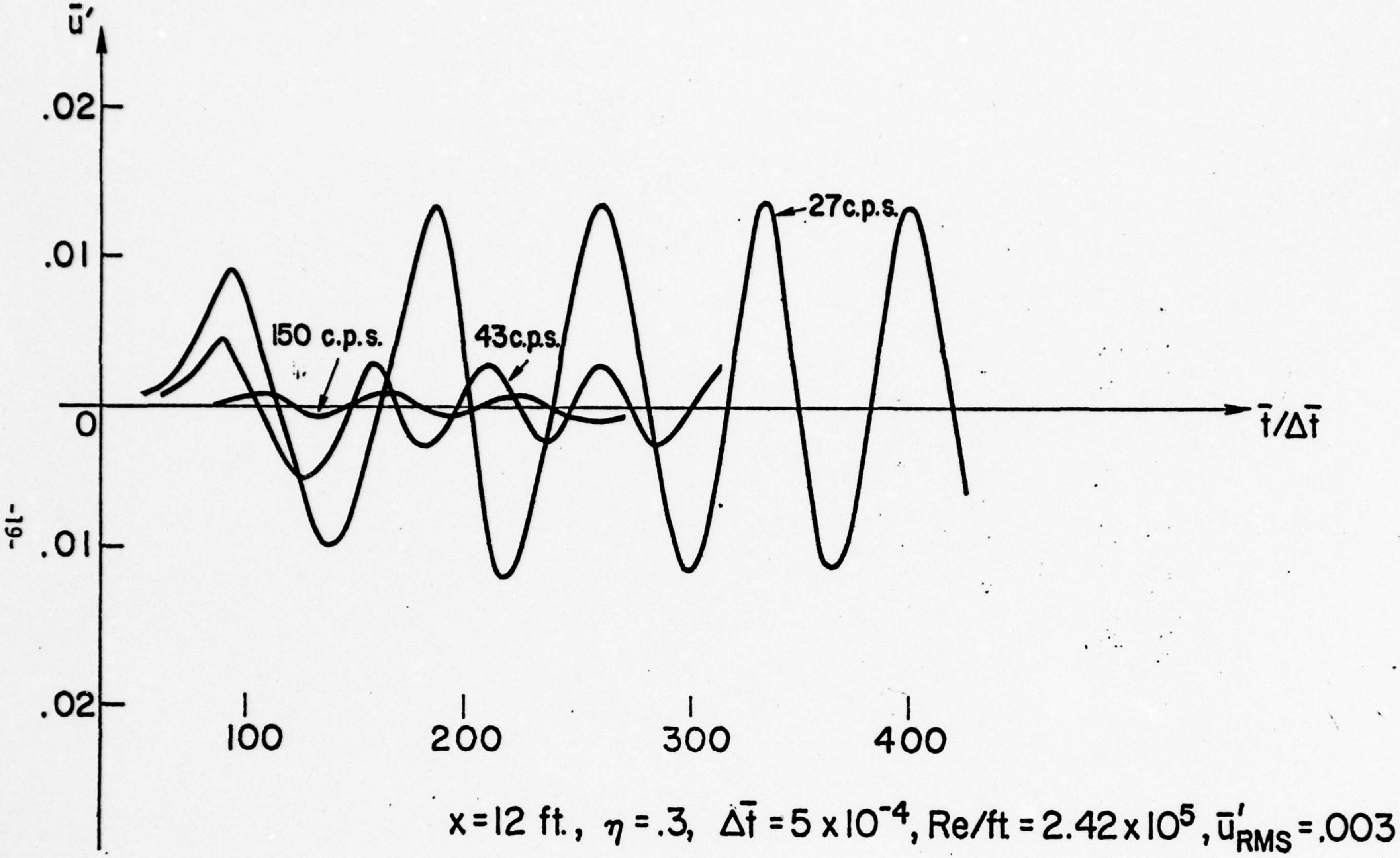

FIGURE 3. FREQUENCY DEPENDENCE ON DAMPING OR AMPLIFICATION OF ACOUSTICAL DISTURBANCE

Figures 4 and 5 present the temporal history, for the 27 cycle/sec case for $U'_{R.M.S.}$ = .3% of freestream at different stations downstream of the leading edge at two different transverse stations. As one moves significantly downstream (i.e., to x = 16 ft) the level of amplification decreases (its maximum is at x = 8 ft, corresponding to an $Re_L = 1.9 \times 10^6$). Such results are in line with previous results, i.e., the amplification curves of Fasel[1] where the amplification increases as one passes into the instability region and decreases as the neutral stability curve is again crossed.

An illustration of severe damping is exhibited in Figure 6, which shows how a large perturbation is damped when the frequency is well outside of stability theory. The exceptionally high value of disturbance is almost completely damped at x = 6 ft.

Much has been said about the effect of acoustics on transition, the application of linear stability theory with the mismatch of propagation velocities between turbulence and acoustic waves, and whether or not Tollmien Schlichting waves are excited under the influence of sound waves. Indeed, the frequency range of the experiments is in line with stability theory. An investigation was initiated to determine what the propagation speed inside the boundary layer was. In all cases, while the disturbances were propagating with the speed of sound along the freestream, the waves within the boundary layer were propagating at a speed of the order of the freestream speed, and thus indeed, the waves are the classical Tollmien Schlichting waves. Such a result is presented in Figure 7. This result is in agreement with the recent experiments reported in Ref. 10.

What is essentially occurring is that the wave propagating along the outer edge has little effect on the boundary layer development. Instead, the major effect is the profile at the leading edge, and thus, the effect of the acoustic wave is only to set up the initial disturbance field (i.e., at $\bar{x} = \bar{x}^*$). Since

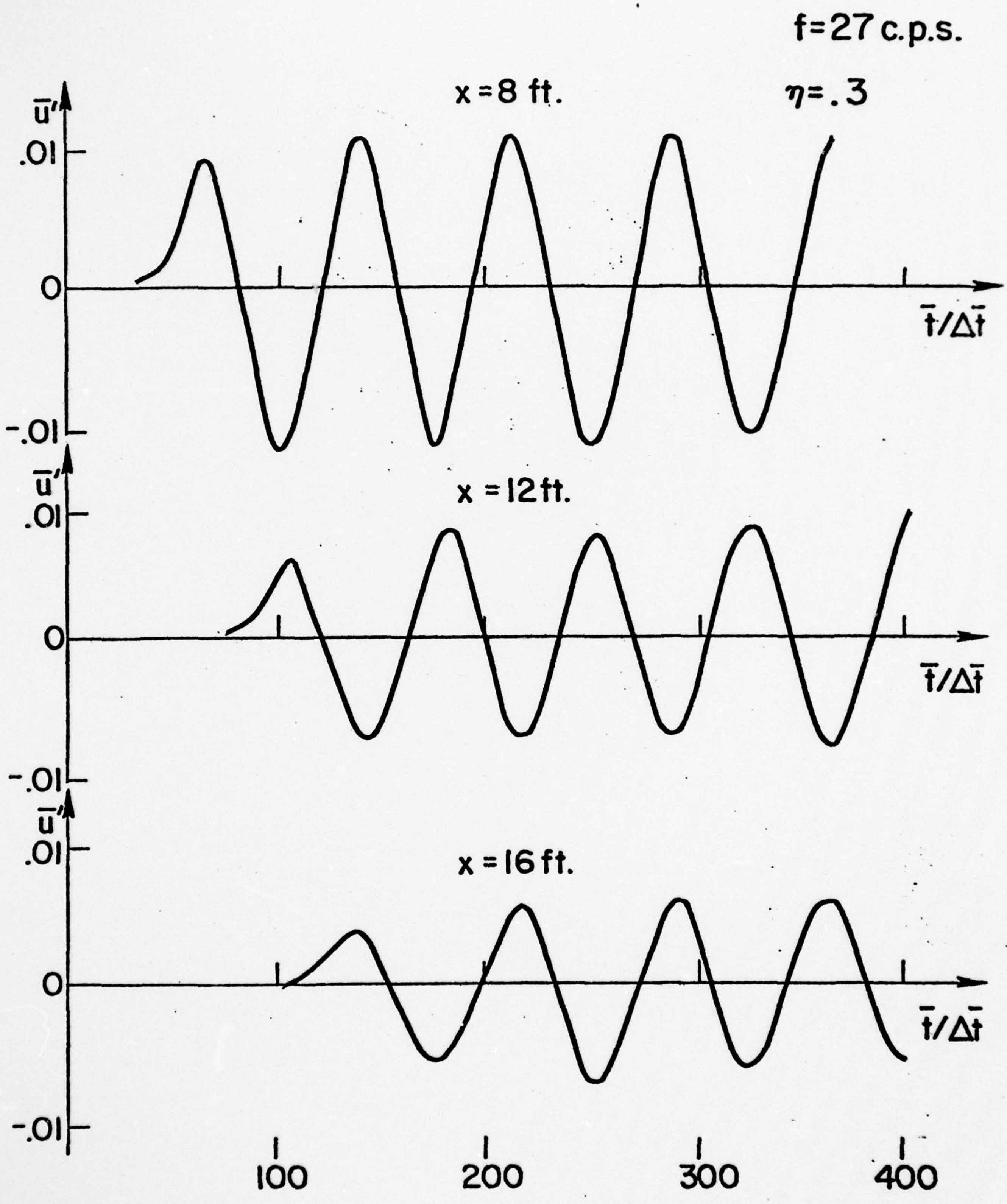

FIGURE 4. TEMPORAL HISTORY DOWNSTREAM OF IMPOSED DISTURBANCE (η = .3, f = 27 cps)

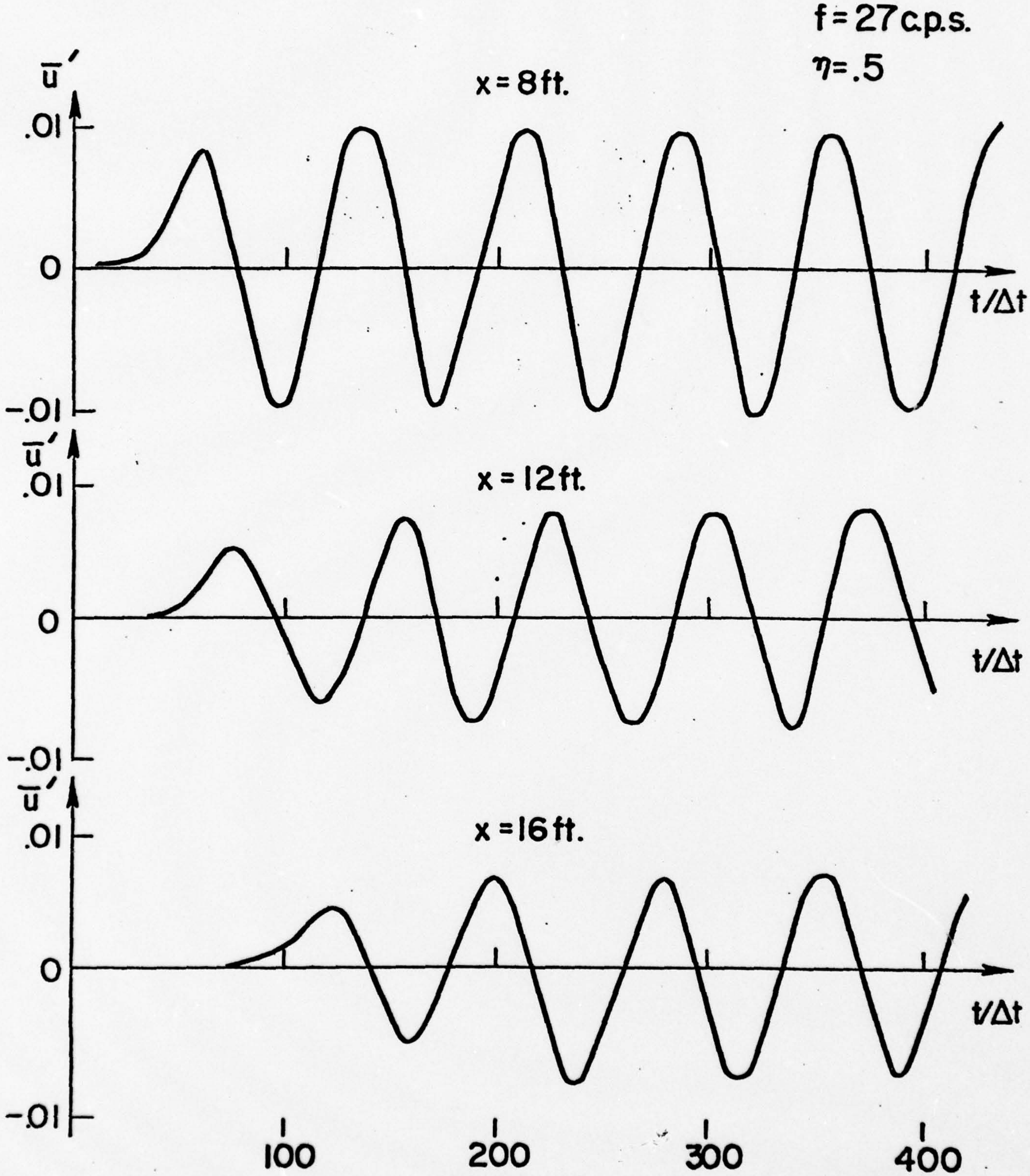

FIGURE 5: TEMPORAL HISTORY DOWNSTREAM OF IMPOSED DISTURBANCE (η = .5, f = 27 cps

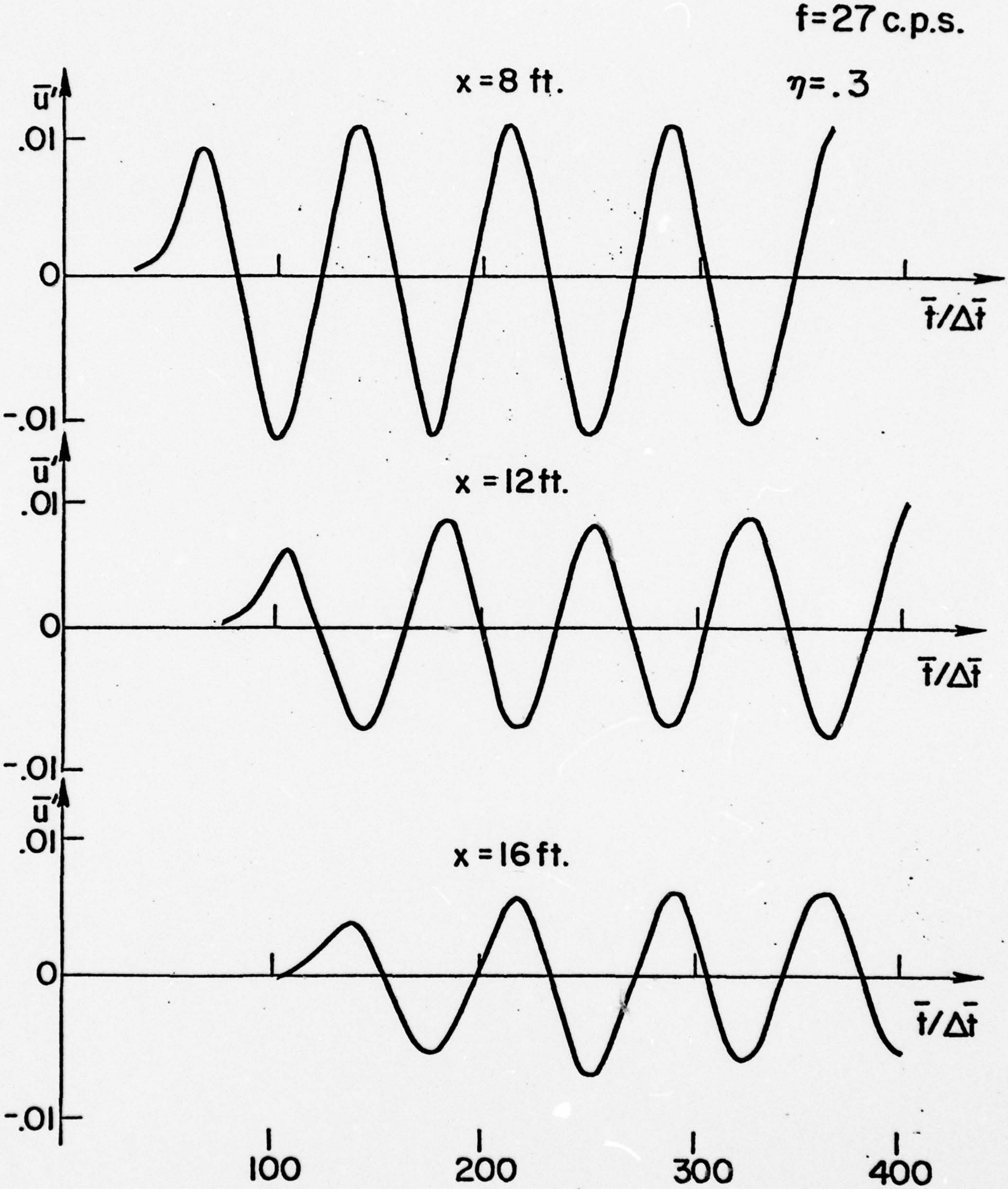

FIGURE 4. TEMPORAL HISTORY DOWNSTREAM OF IMPOSED DISTURBANCE (n = .3, f = 27 cps)

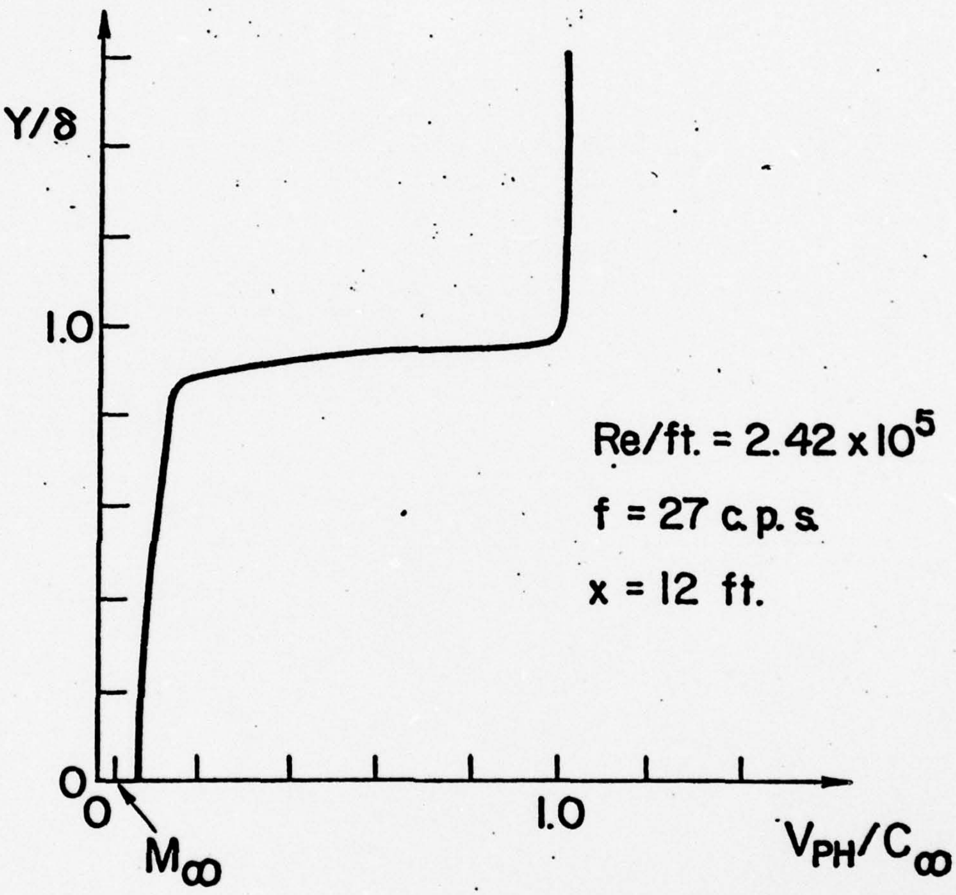

FIGURE 7. PHASE SPEED OF WAVES INSIDE BOUNDARY LAYER UNDER THE INFLUENCE OF ACOUSTICAL DISTURBANCE

we have found that the profiles of References 5 and 6 are representative of the acoustical disturbance profile near the leading edge, the effect of acoustics on transition is, indeed, similar to the effect of other large (or small) perturbations such as the roughness element effects described previously.

In order to test this result, a series of runs were made to compare the results of the present code to those of other investigations. Figures 8 and 9 illustrate how the results of the present analysis compare with the results of Ref. 2. Even though at the outer boundary, waves are propagating at a speed one to two orders of magnitude greater than the freestream velocity, the results of the present investigation with respect to boundary layer response are in good agreement with the results of Ref. 2.

Figure 10 illustrates a test case run to see how the method compares with linear stability theory. For the case $U_\infty/\nu = .6 \times 10^5$/ft and f = 25 cps (with L = 12 ft) linear stability theory predicts that the Reynolds number based on displacement thickness for neutral stability is approximately 1125. For $Re^* < 1125$ waves are damped, for $Re^* > 1125$ waves are amplified. The results of the present calculation indicate this to be the case, again confirming both the utility of the method and the fact that the response of a boundary layer to acoustic vibrations is similar to the response to other disturbance fields.

A remark is necessary with respect to the utility of the present analysis with respect to the problem of transition. There is much question as to the length of the three dimensional region prior to transition. Indeed, if three-dimensional effects predominate over a long distance prior to transition, two dimensional programs will be unable to predict transition accurately. Such a program though, can be of value with respect to determining basic flow structure in regions prior to the onset of transition, as has been demonstrated here.

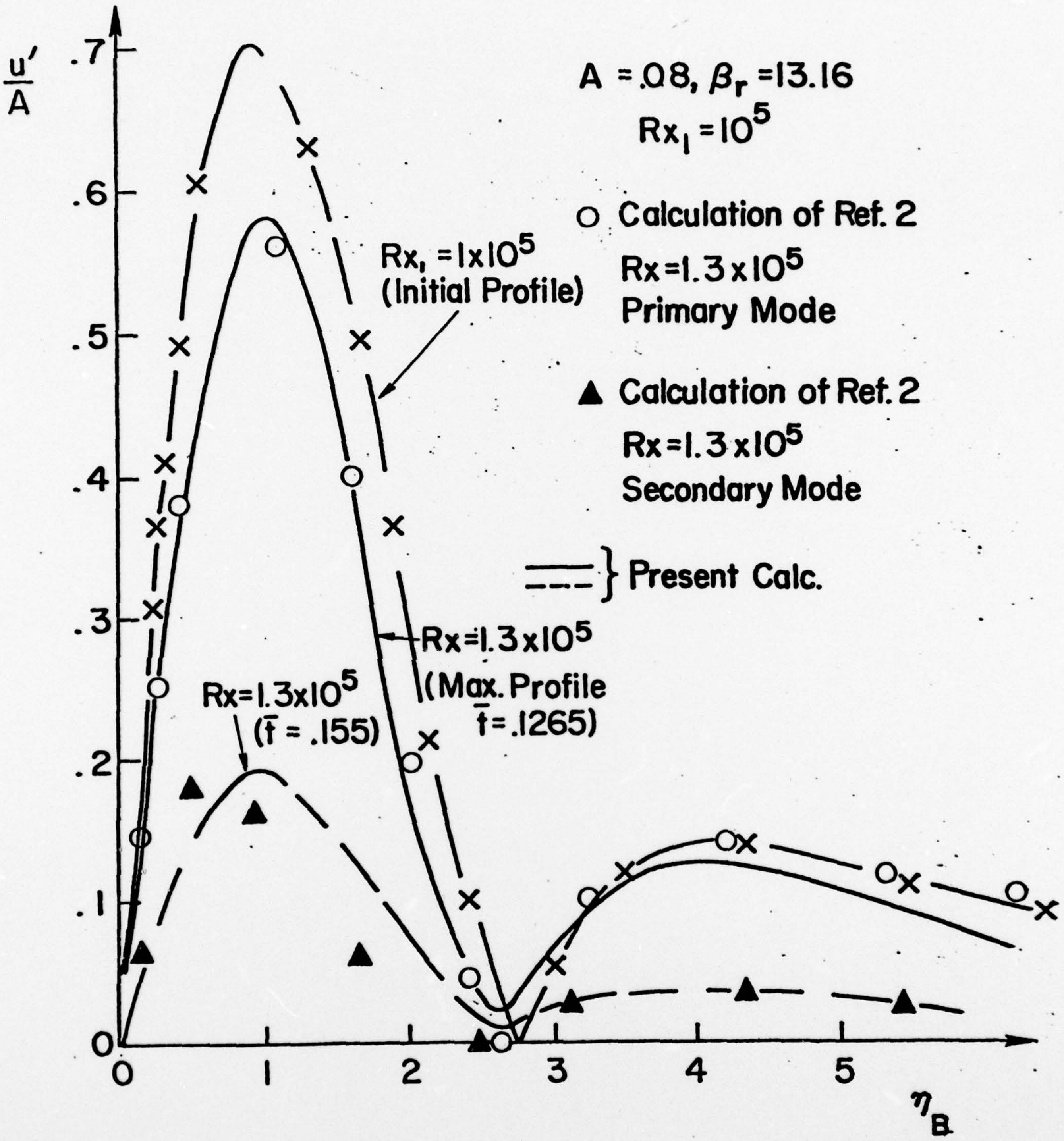

FIGURE 8. COMPARISON OF COMPUTED DISTURBANCE PROFILES WITH DATA OF REFERENCE 2

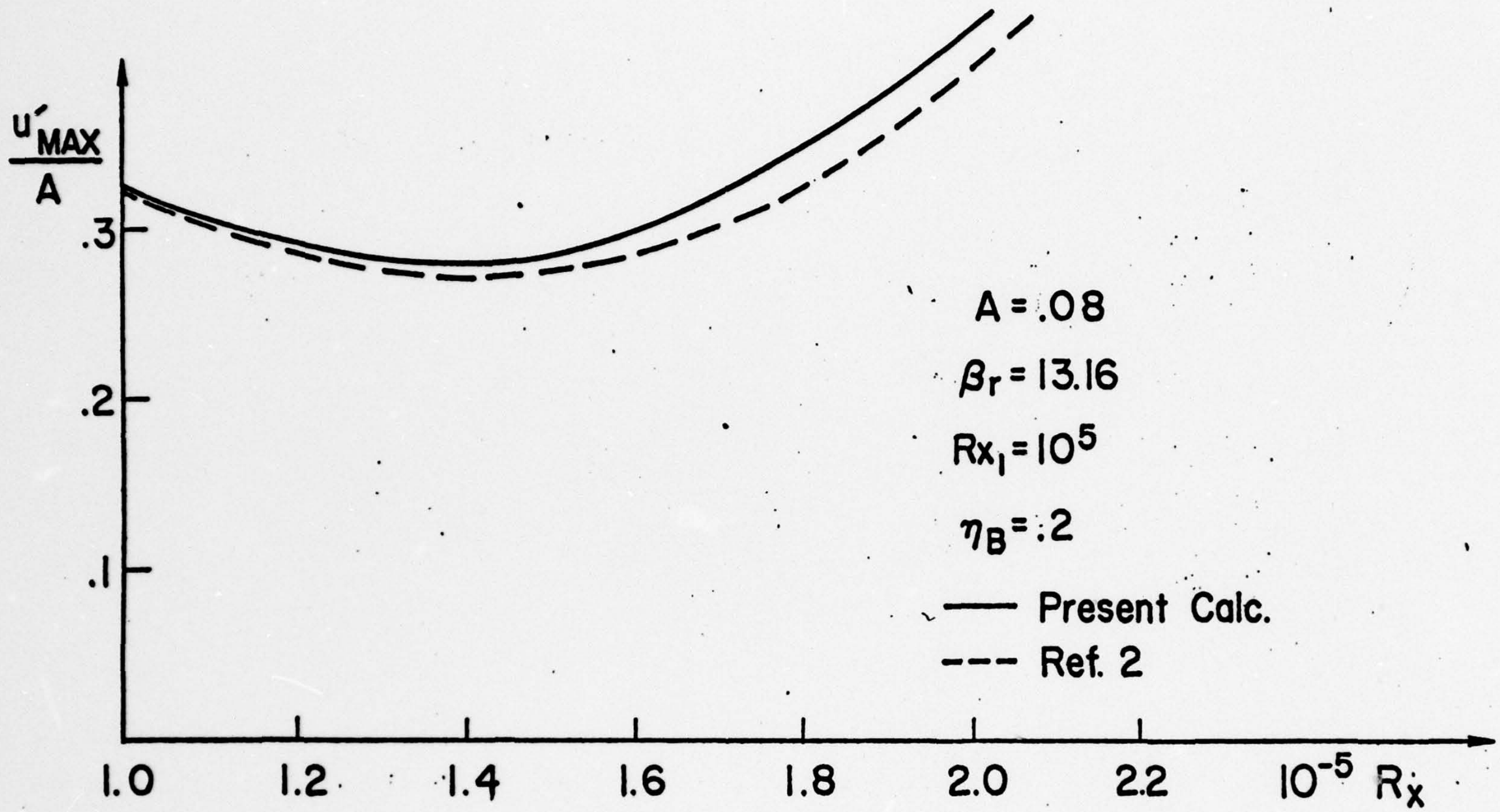

FIGURE 9. COMPARISON OF MAXIMUS DISTURBANCE DISTRIBUTION WITH DATA OF REFERENCE 2

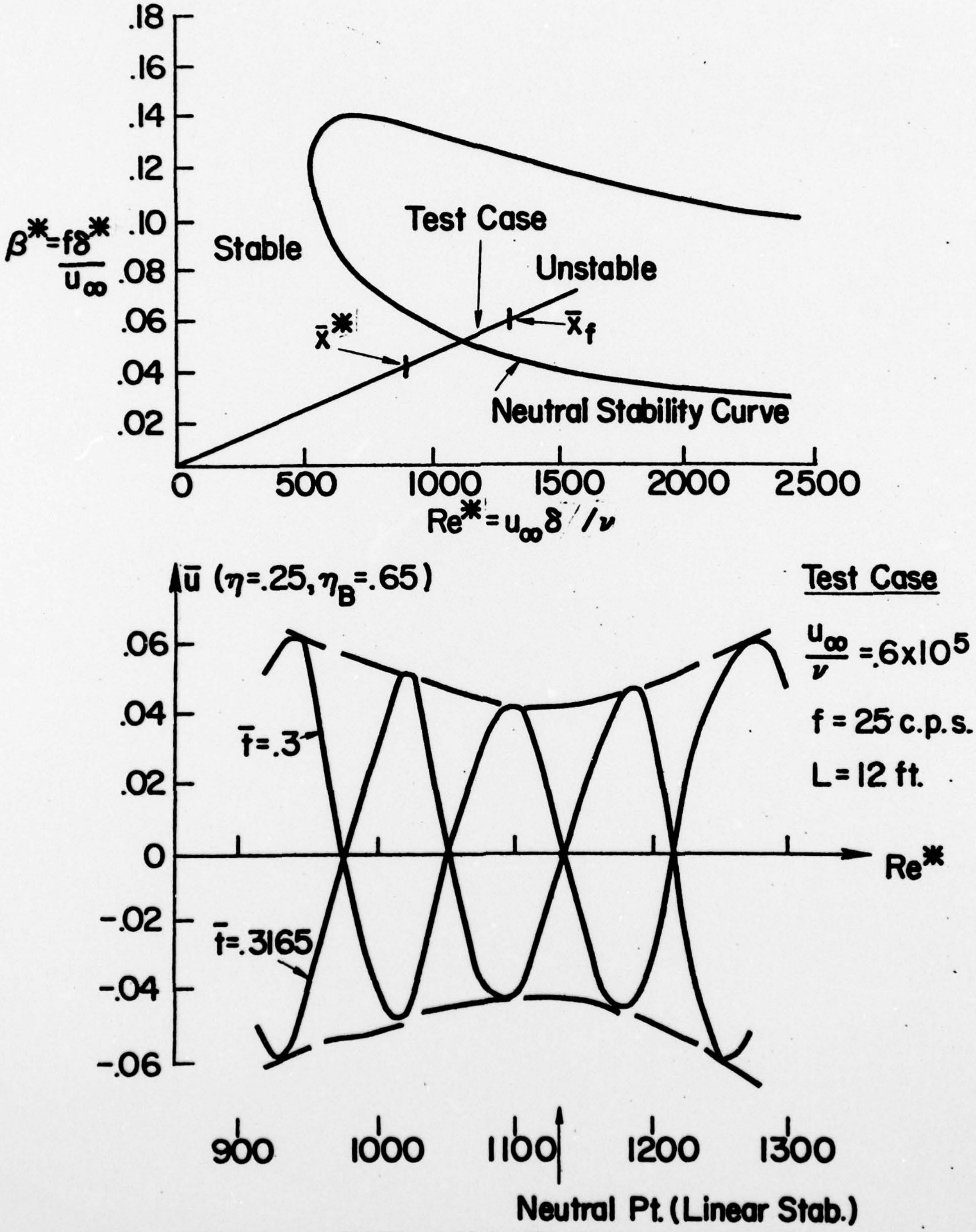

FIGURE 10. COMPARISON OF PROGRAM OUTPUT WITH LINEAR STABILITY THEORY

It is felt that the results achieved to date provide a fundamental understanding with respect to boundary layer response to acoustical disturbances. It seems necessary at this time that the numerical analysis and computer code be modified with respect to the marching step utilized in order to allow the program to have general applicability (for example, to allow the program to be utilized at lower Reynolds numbers). Therefore, in the coming year, the full, compressible, unsteady Navier Stokes equations will be reprogrammed and solved by an explicit MacCormack scheme with time splitting[13]. Thus the small time scale in the normal direction ($\Delta t_y < \Delta y/c$) can be properly accounted for. There are advantages to utilizing an explicit scheme for the complex system to be solved (as opposed to a fully implicit scheme or an A.D.I.). When solving the full compressible Navier Stokes equations, all derivatives in x and y are immediately computed and thus the solution of the full system is no more complex, in principle, than the solution of the boundary layer system. In addition, whereas an implicit scheme allows one to utilize a bigger time step from a stability viewpoint one is still bound by the small time step criterion from the viewpoint of accuracy.

Once the program has been changed to allow for general applicability, the program will be extended so that a wide range of parameters can be varied. The effects of Mach number, type of disturbance, wall temperature, wall suction or injection, and wall compliance will be studied after the program has been properly modified.

IV. REFERENCES

1. Fasel, H., "Investigation of the Stability of Boundary Layers by a Finite Difference Model of the Navier Stokes Equations," *Journal of Fluid Mechanics,* Vol. 78, Part 2, 1976.

2. Murdock, J. W., "A Numerical Study of Nonlinear Effects on Boundary Layer Stability", *A.I.A.A.,* paper 77-127, January 1977.

3. Smith, A.M.O. and Gameroni, N., "Transition, Pressure Gradient and Stability Theory," Douglas Aircraft Report ES-26388, 1956.

4. Mack, L.M., *"Computation of the Stability of the Laminar Compressible Boundary Layer,"* Methods in Computational Physics, Vol. 4, B. Alder, ed., Academic Press, 1965.

5. Wazzan, A.R., Okamura, T.T. and Smith, A.M.O., "Space and Temporal Stability Charts," Douglas Aircraft Report DAC-67086, 1968.

6. Jordinson, R., "The Flat Plate Boundary Layer, Part 1. Numerical Integration of the Orr-Summerfeld Equation", *Journal of Fluid Mechanics,* Vol. 43, Part 4, 1970.

7. Saric, W.S. and Nayfeh, A.H., "Nonparallel Stability of Boundary Layer Flows", *Journal of Physics of Fluids,* Vol. 18, No. 8, August 1975.

8. Stuart, J. T., "Hydrodynamic Stability," *Applied Mechanics Review,* Vol. 18, 1965.

9. Spangler, J.G. and Wells, C.S., "Effects of Freestream Disturbances on Boundary Layer Transition", *Journal of the American Institute of Aeronautics and Astronautics,* Vol. 6, No. 4, 1968.

10. Shapiro, P. J., "The Influence of Sound Upon Laminar Boundary Layer Stability", M.I.T. Rept. No. 83458-83560-1, September 1977.

11. Shubauer,G.B. and Skramstad, H.K., "Laminar Boundary Layer Oscillators and Transition on a Flat Plate", Report 909, NACA, 1948.

12. Miller, G. and Fanchiotti., "An Interaction Model for the Solution of Laminar Separation on a Surface", *A.I.A.A.* paper 75-5, January 1975.

13. MacCormack, R.W., "The Effects of Viscosity in Hypervelocity Impact Cratering", *A.I.A.A.* paper 69-354, 1969.

14. Klebanoff, P.S. and Tidstrom, K.D., "Mechanism by Which a Two-Dimensional Roughness Element Induces Boundary Layer Transition", *Journal of Physics of Fluids,* Vol. 15, No. 7, 1972.

DISTRIBUTION LIST FOR UNCLASSIFIED
TECHNICAL REPORTS AND REPRINTS ISSUED UNDER
CONTRACT N00014-76-C-0183 TASK NR 061-232

All addresses receive one copy unless otherwise specified

Technical Library
Building 313
Ballistic Research Laboratories
Aberdeen Proving Ground, MD 21005

Dr. F. D. Bennett
External Ballistic Laboratory
Ballistic Research Laboratories
Aberdeen Proving Ground, MD 21005

Mr. C. C. Hudson
Sandia Corporation
Sandia Base
Albuquerque, NM 81115

Professor P. J. Roache
Ecodynamics Research
Associates, Inc.
P. O. Box 8172
Albuquerque, NM 87108

Dr. J. D. Shreve, Jr.
Sandia Corporation
Sandia Base
Albuquerque, NM 81115

Defense Documentation Center
Cameron Station, Building 5
Alexandria, VA 22314 12 Copies

Library
Naval Academy
Annapolis, MD 21402

Dr. G. H. Heilmeier
Director, Defense Advanced
Research Projects Agency
1400 Wilson Boulevard
Arlington, VA 22209

Mr. R. A. Moore
Deputy Director, Tactical
Technology Office
Defense Advanced Research Projects
Agency
1400 Wilson Boulevard
Arlington, VA 22209

Office of Naval Research
Code 411
Arlington, VA 22217

Office of Naval Research
Code 421
Arlington, VA 22217

Office of Naval Research
Code 438
Arlington, VA 22217

Office of Naval Research
Code 1021P (ONRL)
Arlington, VA 22217 6 Copies

Dr. J. L. Potter
Deputy Director, Technology
von Karman Gas Dynamics Facility
Arnold Air Force Station, TN 37389

Professor J. C. Wu
Georgia Institute of Technology
School of Aerospace Engineering
Atlanta, GA 30332

Library
Aerojet-General Corporation
6352 North Irwindale Avenue
Azusa, CA 91702

NASA Scientific and Technical
Information Facility
P. O. Box 8757
Baltimore/Washington International Airport
Maryland 21240

Dr. S. A. Berger
University of California
Department of Mechanical Engineering
Berkeley, CA 94720

Professor A. J. Chorin
University of California
Department of Mathematics
Berkeley, CA 94720

Professor M. Holt
University of California
Department of Mechanical Engineering
Berkeley, CA 94720

Dr. L. Talbot
University of California
Department of Mechanical Engineering
Berkeley, CA 94720

Dr. H. R. Chaplin
Code 16
David W. Taylor Naval Ship Research and Development Center
Bethesda, MD 20084

Code 1800
David W. Taylor Naval Ship Research and Development Center
Bethesda, MD 20084

Code 5643
David W. Taylor Naval Ship Research and Development Center
Bethesda, MD 20084

Dr. G. R. Inger
Virginia Polytechnic Institute and State University
Department of Aerospace Engineering
Blacksburg, VA 24061

Professor A. H. Nayfeh
Virginia Polytechnic Institute and State University
Department of Engineering Science and Mechanics
Blacksburg, VA 24061

Indiana University
School of Applied Mathematics
Bloomington, IN 47401

Director
Office of Naval Research Branch Office
495 Summer Street
Boston, MA 02210

Supervisor, Technical Library Section
Thiokol Chemical Corporation
Wasatch Division
Brigham City, UT 84302

Dr. G. Hall
State University of New York at Buffalo
Faculty of Engineering and Applied Science
Fluid and Thermal Sciences Laboratory
Buffalo, NY 14214

Mr. R. J. Vidal
Calspan Corporation
Aerodynamics Research Department
P. O. Box 235
Buffalo, NY 14221

Professor R. F. Probstein
Massachusetts Institute of Technology
Department of Mechanical Engineering
Cambridge, MA 02139

Director
Office of Naval Research Branch Office
536 South Clark Street
Chicago, IL 60605

Code 753
Naval Weapons Center
China Lake, CA 93555

Mr. J. Marshall
Code 4063
Naval Weapons Center
China Lake, CA 93555

Professor R. T. Davis
University of Cincinnati
Department of Aerospace Engineering and Applied Mechanics
Cincinnati, OH 45221

Library MS 60-3
NASA Lewis Research Center
21000 Brookpark Road
Cleveland, OH 44135

Dr. J. D. Anderson, Jr.
Chairman, Department of Aerospace Engineering
College of Engineering
University of Maryland
College Park, MD 20742

Professor W. L. Melnik
University of Maryland
Department of Aerospace Engineering
Glenn L. Martin Institute of Technology
College Park, MD 20742

Professor O. Burggraf
Ohio State University
Department of Aeronautical and
Astronautical Engineering
1314 Kinnear Road
Columbus, OH 43212

Technical Library
Naval Surface Weapons Center
Dahlgren Laboratory
Dahlgren, VA 22448

Dr. F. Moore
Naval Surface Weapons Center
Dahlgren Laboratory
Dahlgren, VA 22448

Technical Library 2-51131
LTV Aerospace Corporation
P. O. Box 5907
Dallas, TX 75222

Library, United Aircraft Corporation
Research Laboratories
Silver Lane
East Hartford, CT 06108

Technical Library
AVCO-Everett Research Laboratory
2385 Revere Beach Parkway
Everett, MA 02149

Professor G. Moretti
Polytechnic Institute of New York
Long Island Center
Department of Aerospace Engineering
and Applied Mechanics
Route 110
Farmingdale, NY 11735

Professor S. G. Rubin
Polytechnic Institute of New York
Long Island Center
Department of Aerospace Engineering
and Applied Mechanics
Route 110
Farmingdale, NY 11735

Technical Documents Center
Army Mobility Equipment R&D Center
Building 315
Fort Belvoir, VA 22060

Dr. W. R. Briley
Scientific Research Associates, Inc.
P. O. Box 498
Glastonbury, CT 06033

Library (MS 185)
NASA Langley Research Center
Langley Station
Hampton, VA 23665

Dr. S. Nadir
Northrop Corporation
Aircraft Division
3901 West Broadway
Hawthorne, CA 90250

Professor A. Chapmann
Chairman, Mechanical Engineering
Department
William M. Rice Institute
Box 1892
Houston, TX 77001

Dr. F. Lane
KLD Associates, Inc.
7 High Street
Huntington, NY 11743

Technical Library
Naval Ordnance Station
Indian Head, MD 20640

Professor D. A. Caughey
Cornell University
Sibley School of Mechanical and
Aerospace Engineering
Ithaca, NY 14853

Professor E. L. Resler
Cornell University
Sibley School of Mechanical and
Aerospace Engineering
Ithaca, NY 14853

Professor S. F. Shen
Cornell University
Sibley School of Mechanical and
Aerospace Engineering
Ithaca, NY 14853

Library
Midwest Research Institute
425 Volker Boulevard
Kansas City, MO 64110

Dr. M. M. Hafez
Flow Research, Inc.
P. O. Box 5040
Kent, WA 98031

Dr. E. M. Murman
Flow Research, Inc.
P. O. Box 5040
Kent, WA 98031

Dr. S. A. Orszag
Cambridge Hydrodynamics, Inc.
54 Baskin Road
Lexington, MA 02173

Professor T. Cebeci
California State University. Long Beach
Mechanical Engineering Department
Long Beach, CA 90840

Mr. J. L. Hess
Douglas Aircraft Company
3855 Lakewood Boulevard
Long Beach, CA 90808

Dr. H. K. Cheng
University of Southern California,
University Park
Department of Aerospace Engineering
Los Angeles, CA 90007

Professor J. D. Cole
University of California
Mechanics and Structures Department
School of Engineering and Applied
Science
Los Angeles, CA 90024

Engineering Library
University of Southern California
Box 77929
Los Angeles, CA 90007

Dr. C. -M. Ho
University of Southern California,
University Park
Department of Aerospace Engineering
Los Angeles, CA 90007

Dr. T. D. Taylor
The Aerospace Corporation
P. O. Box 92957
Los Angeles, CA 90009

Commanding Officer
Naval Ordnance Station
Louisville, KY 40214

Mr. B. H. Little, Jr.
Lockheed-Georgia Company
Department 72-74, Zone 369
Marietta, GA 30061

Dr. C. Cook
Stanford Research Institute
Menlo Park, CA 94025

Professor E. R. G. Eckert
University of Minnesota
241 Mechanical Engineering Building
Minneapolis, MN 55455

Library
Naval Postgraduate School
Monterey, CA 93940

McGill University
Supersonic-Gas Dynamics Research
Laboratory
Department of Mechanical Engineering
Montreal 12, Quebec, Canada

Librarian
Engineering Library, 127-223
Radio Corporation of America
Morristown, NJ 07960

Dr. S. S. Stahara
Nielsen Engineering & Research, Inc.
510 Clyde Avenue
Mountain View, CA 94043

Engineering Societies Library
345 East 47th Street
New York, NY 10017

Professor A. Jameson
New York University
Courant Institute of Mathematical
Sciences
251 Mercer Street
New York, NY 10012

Professor G. Miller
New York University
Department of Applied Science
26-36 Stuyvesant Street
New York, NY 10003

Office of Naval Research
New York Area Office
715 Broadway - 5th Floor
New York, NY 10003

Dr. A. Vaglio-Laurin
New York University
Department of Applied Science
26-36 Stuyvesant Street
New York, NY 10003

Professor S. Weinbaum
Research Foundation of the City
University of New York on behalf
of the City College
1411 Broadway
New York, NY 10018

Librarian, Aeronautical Library
National Research Council
Montreal Road
Ottawa 7, Canada

Lockheed Missiles and Space Company
Technical Information Center
3251 Hanover Street
Palo Alto, CA 94304

Director
Office of Naval Research Branch Office
1030 East Green Street
Pasadena, CA 91106

California Institute of Technology
Engineering Division
Pasadena, CA 91109

Library
Jet Propulsion Laboratory
4800 Oak Grove Drive
Pasadena, CA 91103

Professor H. Liepmann
California Institute of Technology
Department of Aeronautics
Pasadena, CA 91109

Mr. L. I. Chasen, MGR-MSD Lib.
General Electric Company
Missile and Space Division
P. O. Box 8555
Philadelphia, PA 19101

Mr. P. Dodge
Airesearch Manufacturing Company
of Arizona
Division of Garrett Corporation
402 South 36th Street
Phoenix, AZ 85034

Technical Library
Naval Missile Center
Point Mugu, CA 93042

Professor S. Bogdonoff
Princeton University
Gas Dynamics Laboratory
Department of Aerospace and
Mechanical Sciences
Princeton, NJ 08540

Professor S. I. Cheng
Princeton University
Department of Aerospace and
Mechanical Sciences
Princeton, NJ 08540

Dr. J. E. Yates
Aeronautical Research Associates
of Princeton, Inc.
50 Washington Road
Princeton, NJ 08540

Professor J. H. Clarke
Brown University
Division of Engineering
Providence, RI 02912

Professor J. T. C. Liu
Brown University
Division of Engineering
Providence, RI 02912

Professor L. Sirovich
Brown University
Division of Applied Mathematics
Providence, RI 02912

Dr. P. K. Dai (R1/2178)
TRW Systems Group, Inc.
One Space Park
Redondo Beach, CA 90278

Redstone Scientific Information Center
Chief, Document Section
Army Missile Command
Redstone Arsenal, AL 35809

U.S. Army Research Office
P. O. Box 12211
Research Triangle, NC 27709

Professor M. Lessen
The University of Rochester
Department of Mechanical Engineering
River Campus Station
Rochester, NY 14627

Editor, Applied Mechanics Review
Southwest Research Institute
8500 Culebra Road
San Antonio, TX 78228

Library and Information Services
General Dynamics-CONVAIR
P. O. Box 1128
San Diego, CA 92112

Dr. R. Magnus
General Dynamics-CONVAIR
Kearny Mesa Plant
P. O. Box 80847
San Diego, CA 92138

Mr. T. Brundage
Defense Advanced Research Projects Agency
Research and Development Field Unit
APO 146, Box 271
San Francisco, CA 96246

Office of Naval Research
San Francisco Area Office
760 Market Street - Room 447
San Francisco, CA 94102

Library
The Rand Corporation
1700 Main Street
Santa Monica, CA 90401

Department Librarian
University of Washington
Department of Aeronautics and Astronautics
Seattle, WA 98105

Dr. P. E. Rubbert
Boeing Commercial Airplane Company
P. O. Box 3707
Seattle, WA 98124

Mr. R. Feldhuhn
Naval Surface Weapons Center
White Oak Laboratory
Silver Spring, MD 20910

Dr. G. Heiche
Naval Surface Weapons Center
Mathematical Analysis Branch
Silver Spring, MD 20910

Librarian
Naval Surface Weapons Center
White Oak Laboratory
Silver Spring, MD 20910

Dr. J. M. Solomon
Naval Surface Weapons Center
White Oak Laboratory
Silver Spring, MD 20910

Professor J. H. Ferziger
Stanford University
Department of Mechanical Engineering
Stanford, CA 94305

Professor K. Karamcheti
Stanford University
Department of Aeronautics and Astronautics
Stanford, CA 94305

Professor M. van Dyke
Stanford University
Department of Aeronautics and Astronautics
Stanford, CA 94305

Engineering Library
McDonnell Douglas Corporation
Department 218, Building 101
P. O. Box 516
St. Louis, MO 63166

Dr. R. J. Hakkinen
McDonnell Douglas Corporation
Department 222
P. O. Box 516
St. Louis, MO 63166

Dr. R. P. Heinisch
Honeywell, Inc.
Systems and Research Division -
Aerospace Defense Group
2345 Walnut Street
St. Paul, MN 55113

Professor R. G. Stoner
Arizona State University
Department of Physics
Tempe, AZ 85721

Dr. N. Malmuth
Rockwell International
Science Center
1049 Camino Dos Rios
P. O. Box 1085
Thousand Oaks, CA 91360

Rockwell International
Science Center
1049 Camino Dos Rios
P. O. Box 1085
Thousand Oaks, CA 91360

The Library
University of Toronto
Institute of Aerospace Studies
Toronto 5, Canada

Professor W. R. Sears
University of Arizona
Aerospace and Mechanical Engineering
Tucson, AZ 85721

Professor A. R. Seebass
University of Arizona
Department of Aerospace and
Mechanical Engineering
Tucson, AZ 85721

Dr. S. M. Yen
University of Illinois
Coordinated Science Laboratory
Urbana, IL 61801

Dr. K. T. Yen
Code 3015
Naval Air Development Center
Warminster, PA 18974

Air Force Office of Scientific
Research (SREM)
Building 1410, Bolling AFB
Washington, DC 20332

Chief of Research & Development
Office of Chief of Staff
Department of the Army
Washington, DC 20310

Library of Congress
Science and Technology Division
Washington, DC 20540

Director of Research (Code RR)
National Aeronautics and
Space Administration
600 Independence Avenue, SW
Washington, DC 20546

Library
National Bureau of Standards
Washington, DC 20234

National Science Foundation
Engineering Division
1800 G Street, NW
Washington, DC 20550

Mr. W. Koven (AIR 03E)
Naval Air Systems Command
Washington, DC 20361

Mr. R. Siewert (AIR 320D)
Naval Air Systems Command
Washington, DC 20361

Technical Library Division (AIR 604)
Naval Air Systems Command
Washington, DC 20361

Code 2627
Naval Research Laboratory
Washington, DC 20375

SEA 03512
Naval Sea Systems Command
Washington, DC 20362

SEA 09G3
Naval Sea Systems Command
Washington, DC 20362

Dr. A. L. Slafkosky
Scientific Advisor
Commandant of the Marine Corps
(Code AX)
Washington, DC 20380

Director
Weapons Systems Evaluation Group
Washington, DC 20305

Dr. P. Baronti
General Applied Science
Laboratories, Inc.
Merrick and Stewart Avenues
Westbury, NY 11590

Bell Laboratories
Whippany Road
Whippany, NJ 07981

Chief of Aerodynamics
AVCO Corporation
Missile Systems Division
201 Lowell Street
Wilmington, MA 01887

Research Library
AVCO Corporation
Missile Systems Division
201 Lowell Street
Wilmington, MA 01887

AFAPL (APRC)
AB
Wright Patterson, AFB, OH 45433

Dr. Donald J. Harney
AFFDL/FX
Wright Patterson AFB, OH 45433